

FT-IR and Raman spectroscopy for the study of amber and other fossil resins

Gintarė Martinkutė-Baranauskienė¹,

Martynas Talaikis²,

Petras Šinkūnas¹,

Jonas Kiuberis³

¹*Institute of Geosciences,
Faculty of Chemistry and Geosciences,
Vilnius University,
21 M. K. Čiurlionio Street, Vilnius*

²*Center for Physical Sciences
and Technology,
3 Saulėtekio Avenue, Vilnius*

³*Institute of Chemistry,
Faculty of Chemistry and Geosciences,
Vilnius University,
24 Naugarduko Street, Vilnius*

This study compares the FT-IR and Raman spectra of amber and other fossil resins from different world regions. The spectra of those resins were analysed based on absorption bands related to the vibrational frequencies of various functional groups present in these compounds. Both spectroscopic methods, FT-IR and Raman, are well-suited for the non-destructive identification of various fossil resins. It was found that FT-IR spectroscopy is particularly suitable for identifying Baltic amber due to its characteristic peak in the 1250–1175 cm⁻¹ wavelength region. Raman spectroscopy can provide helpful information regarding the degree of maturation of resins. The presence of specific Raman bands, such as 1771–1543 and 1510–1400 cm⁻¹, as well as 745 and 696 cm⁻¹, can help determine not only the resin's maturity but also any structural changes that occurred during burial over the geological time of different lengths.

Keywords: amber, fossil resins, maturation, burial conditions, spectral characteristics

INTRODUCTION

In this study, the term *fossil resin* is used as a general term for all mature resins, except for the Baltic material under investigation, which is referred to as *amber*. Amber, along with other fossil resins, is precious in analysing the geological history of our planet. Resins originating from the viscous exudates of trees undergo complex transformations over time, eventually forming solid, fossilised materials that we study today. Understanding factors such as deposition conditions, polymerisation, fossilisation processes, and the maturation level of fossil resins is essential to grasping their geological significance.

Ambers and other fossil resins are of different ages, originate from different botanical sources, accumulate in various environments and climates, and are buried under different geological conditions, resulting in distinct chemical and physical properties.

The Py-GC/MS studies performed by Anderson [2–4] led to the attribution of fossil resins into five classes. This classification is based on the major elements of amber determined by Py-GC/MS and has been applied to fossil resin studies. Fossil resins were classified into five classes based on their basic pyrolysis product differences [4]. The ambers from those classes mainly contain polymerised labdanes in various configurations (classes Ia, Ib, Ic), polymerised sesquiterpenes

* Corresponding author. Email: gintare.martinkute@chgf.stud.vu.lt

with triterpenes (class II), polymerised polystyrenes (III), non-polymeric sesquiterpenes (IV) and non-polymeric dicarboxylic acids (V).

FT-IR and Raman spectroscopy, when used together, typically provide excellent results in analysing organic, polymeric, and in some cases, inorganic materials. This combination enables the identification of the relationship between resin formation mechanisms, botanical sources, and the physical and chemical properties of the resins. Significant progress has been made in the study of resins using these analytical methods over the past few decades [8].

The most widely used analytical technique for the identification and chemical characterisation of amber is Fourier Transform Infrared (FT-IR) spectroscopy [7, 16]. This method is particularly popular due to the fact that FT-IR instruments are widely available, easy to use, and allow for very rapid analysis. A significant advantage of the device is its ability to provide reliable data from a small amount of material. FT-IR spectra of the resins are analysed based on absorption bands related to the vibrational frequencies of various chemical groups in the 4000–1450 cm^{-1} region. Additionally, valuable information is obtained by analysing the so-called ‘fingerprint’ region (1450–600 cm^{-1}) [10, 21, 9, 20].

In 1965, C. W. Beck identified a characteristic peak in the 1250–1175 cm^{-1} wavelength region in the FT-IR spectrum and a peak in the 1150 cm^{-1} region (C–O), which he referred to as the ‘Baltic shoulder’. Since then, the characteristic peaks in the 1250–1175 cm^{-1} region of FT-IR spectra have been considered the ‘fingerprints’ of Baltic amber, while the peak in the 1150 cm^{-1} region indicates the position of the C–O group. The peak in the 1600 cm^{-1} region, corresponding to the position of the C–C group, becomes apparent during amber oxidation. It is believed that during oxidation, conjugated double bonds transform into isolated double bonds [19].

Raman spectroscopy, like FT-IR, is also well-suited for non-destructive analysis. The most prominent features in all spectra appear around the 1640 and 1440 cm^{-1} regions. Copal can be distinguished from amber by the intensity ratio of signals at 1640 and 1450 cm^{-1} (I1646/I1450). This ratio can be interpreted as the degree of polymerisation and/or cyclization process that may

occur during the diagenetic transformation of the resin [8, 5].

Like infrared spectra, Raman spectra also allow for grouping resins of similar chemical composition, narrowing down their geographical and botanical origins. However, spectral differences between various samples are often subtle and can be influenced by impurities, aging, or processing methods [8, 17].

MATERIALS AND METHODS

Twelve fossil resin samples of different ages from different locations were collected for the study. Table 1 describes the collected resin samples.

Raman measurements were performed at the Center for Physical Sciences and Technology in Vilnius. They were conducted using a BRUKER MultiRaman spectrometer with a laser wavelength of 1064 nm. The spectra were recorded with a resolution of 4 cm^{-1} , laser power of 400 mW, and a sample scanning time of 200 scans.

FT-IR measurements were conducted at the Gemstone Research Laboratory of the Lithuanian Assay Office in Vilnius. A Gemmo FT-IR spectrometer, operating at a spectral resolution of 4 cm^{-1} , was used for the analysis, with 200 scans accumulated per measurement. For comparison purposes, three replicate spectra were collected from each sample. All spectra were processed using the OPUS and Origin software.

RESULTS AND DISCUSSION

Raman spectroscopy

Table 2 presents the wavenumber positions of the bands and their vibrational assignments in the Raman spectra of amber and other fossil resin samples. Figures 1 and 2 display the Raman spectra of all twelve fossil resins under study. The replicate spectra were similar for all samples.

For the analysis of results, the examined resins were grouped based on their botanical source – into coniferous and deciduous trees – and within those groups, they were sorted by age, from the oldest to the youngest ones (Table 3).

Upon comparing the spectra of all fossil resins (Figs 1 and 2) in a wavenumber range of 3200–2600 cm^{-1} , it is observed that the spectra are quite similar.

Table 1. Characteristics of the studied fossil resins

Geographical origin	Age	Botanical source
Italian Dolomites	Upper Triassic 230 Ma	Cheirelepidiaceae (?)
Lebanon, Jezzine	Lower Cretaceous/Upper Barremian ca 125 Ma	Araucarian tree/Agathis levantensis
Jordan	Lower Cretaceous 125 Ma	Agathis
Japan, Kuji	Late Cretaceous/probably Coniacian or Campanian 80–90 Ma	Araucaria, family of Araucariaceae
French, Oise	Eocene ca 53 Ma	Aulacoxylonspar nacense or Leguminosae Caesalpinaceae
China, Liaoning	Lower Eocene 50–53 Ma	Cupressaceous trees
Ukraine, Rivne	Upper Eocene 40.4 Ma	Sciadopityaceae
Mexico, Chiapas	Lower Miocene – Middle Miocene 22.5–26 Ma	Extinct Hymenaea mexicana
Dominican Republic, West Cordillera	Late Oligocene/Early Miocene 20–25 Ma	Hymenaea protera
Nicaragua	Early Miocene 18–23 Ma	Hymenaea tree
Malaysia, Borneo, Sarawak west.	Neogene/Miocene; Middle Miocene 15–17 Ma	Dipterocarpaceae (?)
Madagascar	Holocene from 10,000 to 50,000 years	Hymenaea verrucosa

The samples belong to Kazimieras Mizgiris.

Table 2. Approximate assignment of the vibrational mode for the Raman spectra of fossil resins. Abbreviations: w, weak; vw, very weak; vvw, very very weak; sh, shoulder; m, medium; s, strong; δ , deformation; t, twisting; ρ , rocking; sym, symmetric; asym, asymmetric; v, stretching

Italian Dolomites	Jordan	Lebanon, Jezzine	Japan, Kuji	China, Liaoning	Ukraine, Rivne	French, Oise	Mexico, Chiapas	Dominica, West Cordillera	Nicaragua	Malaysia, Borneo	Madagascar	Approximate assignment of vibrational mode
2926 s	2926 s	2924 s	2926 s	2930 s	2928 s	2930 s	2922 s	2928 s	2928 s	2935 s	2930 s	vasym(CH ₂)
2870 m	2868 m	2870 m	2868 m	2870 m	2872 m	2870 m	2870 m	2868 m	2870 m	2874 m	2872 m	vsym(CH ₃)
2851 w, sh	2849 w, sh	2849 w, sh	2851 vw, sh	2849 w, sh	2849 w, sh	2849 vw, sh		2849 w	2849 w, sh		2851 w, sh	vsym(CH ₂)
1651 ms	1657 ms	1657 ms	1653 ms	1653 ms	1647 ms	1647 s	1651 ms	1645 s	1647 ms	1657 ms	1649 ms	v(C=C)
1450 s	1450 s	1450 s	1450 s	1450 s	1443 s	1443 s	1445 s	1445 s	1441 s	1458 s	1450 s	δ (CH ₂), δ (CH ₃)
1358 m	1358 m	1356 m	1356 m	1352 m	1358 m							δ (CH ₂), δ (CH ₃)
		1300 m	1310 w							1315 m	1315 w	δ (CH ₂), δ (CH ₃)
1302 m	1300 m			1298 m	1298 m	1300 m	1296 m	1296 m	1296 m		1300 w	t(CH ₂), t(CH ₃)
1211 m	1207 m	1207 m	1203 m	1200 w	1203 m	1202 m	1205 m	1203 m	1203 m	1198 vw	1205 w	δ (CCH), δ (C-O)
974 m	976 m	976 m	972 w	978 m	980 m	980 m	976 w	980 m	980 m		976 w	ρ (CH ₂), ρ (CH ₃)
	928 m		937 w	928 m	935 w		935 m					ρ (CH ₂)
					744 m	744 m	748 vw, sh	744 m	744 w, sh	744 m		v(CC)
721 m	727 w		723 m			725 w, sh	721 m	721 m	721 m			v(CC)
	712 w	719 m		710 m	716 m						716 w	v(CC)
					694 w, sh	698 w	698 vw, sh	696 m	696 w, sh	698 vw, sh		
			555 m	557 w		557 m	557 m	555 m	555 m	563 w		δ (CCO)
		538 m		532 m	546 w							
501 m	501 m	505 m									503 w	v(S-S); v(COC)
		453 m	459 w		453 m					457 w	453 w	δ (CCO)
						444 m	447 m	444 m	444 m			

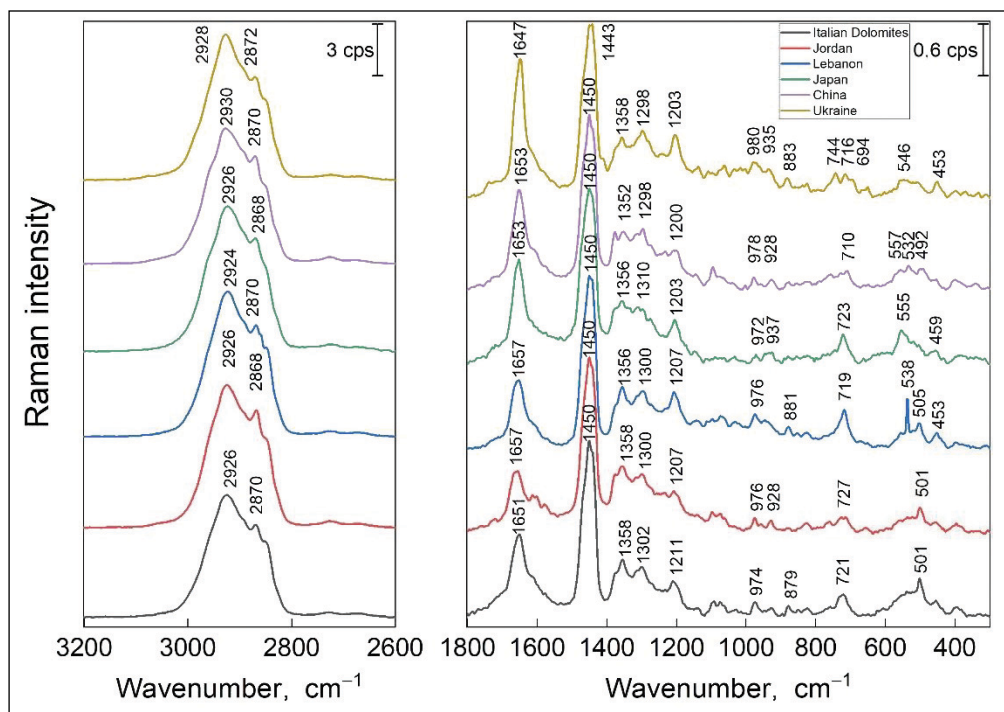


Fig. 1. Raman spectra of fossil resins from coniferous trees

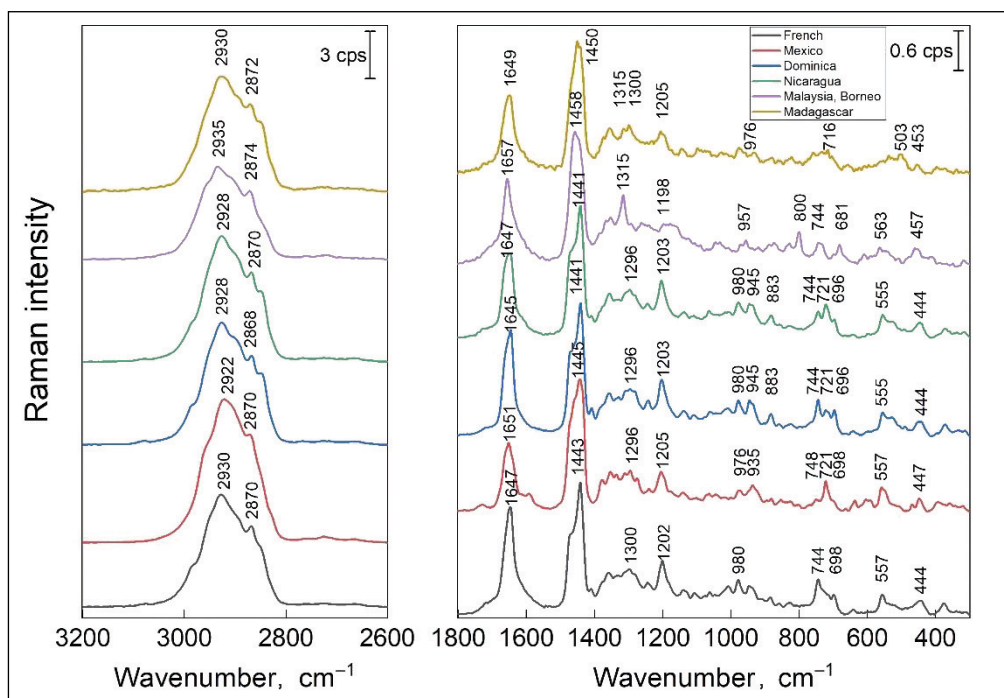


Fig. 2. Raman spectra of fossil resins from deciduous trees

From the obtained data, we can see (Table 2) that the spectral band at 1645–1657 cm^{-1} is assigned to the stretching vibration of carbon–carbon double bond $\nu(\text{C}=\text{C})$, bands at approximately 2850, 2870 and 2928 cm^{-1} are assigned to symmetric methylene, symmetric methyl, and asymmetric

methyl stretching vibrations, respectively. Whereas the modes at 1450 cm^{-1} belong to scissoring and modes at 1300 cm^{-1} to twisting deformations of CH_2 and CH_3 .

Among coniferous trees, Ukrainian amber stands out most of all with a visible triplet at 744,

716 and 694 cm^{-1} in a Raman spectrum wavenumber range of 780–680 cm^{-1} . These bands are here assigned to $\nu(\text{CC})$ modes. In this spectral wavenumber region, the spectral lines of Chinese, Japanese, Lebanese, Jordanian and Italian Dolomite resins in the fingerprint region are clearly different from those of Ukrainian amber.

The spectra of Italian Dolomites, Lebanon, Japan and Mexico show only one sharp peak at 721, 719, 723 and 721 cm^{-1} , respectively. The peaks of Jordan, China and Madagascar resins are of a weak intensity in this area. These bands are here also assigned to $\nu(\text{CC})$ modes.

The spectrum of resin from Dominica is very similar to the spectrum of Ukrainian amber. It also shows a triplet at 744, 721 and 696 cm^{-1} in the wavenumber region 780–680 cm^{-1} .

Since the ratio of bands shown at approximately 1650 and 1450 cm^{-1} has been suggested as an indicator of sample maturity [15], average band intensity ratio values were calculated from each spectrum of the fossil resin collected in this study. The ratios were calculated by measuring the band areas in the wavenumber regions, approximately 1771–1543 and 1510–1400 cm^{-1} . The obtained data are presented in Table 3.

According to the data presented in Table 3, we see that the older the resin, the smaller the ratio of the spectral band areas. The age of the Jordanian

and Lebanese resins is the same and their area ratio $A(1650)/A(1450)$ is very similar. Ukrainian amber is the youngest of the coniferous trees – its area ratio is 1.07. Although the Italian Dolomite resin is the oldest – about 230 million years old, its measured area ratio is 0.81. It may be related to the fact that Italian Dolomite resin belongs to Class II, unlike other resins.

When analysing deciduous tree resins, the highest value of the area ratio in the wavenumber regions 1650 and 1450 cm^{-1} is found in the spectrum of the French resin (1.13), and the lowest value is found in the spectrum of the resin from Mexico (0.59). The area ratio values of the spectra of the resin sample from the Dominican Republic are very similar to the area ratios of the resin samples from Ukraine and Malaysia. According to scientists, the values of the copal and amber samples can be related to their geological age [8].

In amber spectra, the 1450 cm^{-1} band is more intense than 1646 cm^{-1} , while in copal (immature fossil resin) spectra the opposite is true. The relative intensity of the $\nu(\text{C}=\text{C})$ mode at approximately 1646 cm^{-1} decreases as the resin matures, and the degree of resin unsaturation decreases due to processes such as oxidation [8]. This trend is particularly well observed in Fig. 1. The intensity of the 1651 cm^{-1} band in the Italian Dolomite resin is much weaker than that at 1450 cm^{-1} , while

Table 3. The ratio of areas $A(1650)/A(1450)$ and intensities $I(1650)/I(1450)$ of the studied resins

Geographical origin	Class*	Age	$A(1650)/A(1450)$	$I(1650)/I(1450)$	Type of trees
Italian Dolomites	II	230 Ma	0.81	0.46	Conifers
Jordan	Ib	125 Ma	0.61	0.34	Conifers
Lebanon, Jezzine	Ib	125 Ma	0.63	0.40	Conifers
Kuji, Japan	Ib	80–90 Ma	0.74	0.591	Conifers
China, Liaoning	Ib	50–53 Ma	0.84	0.57	Conifers
Ukraine, Rivne	Ia	40.4 Ma	1.07	0.80	Conifers
French, Oise	Ib	53 Ma	1.13	0.82	Deciduous
Mexico, Chiapas	Ic	22.5–26 Ma	0.59	0.52	Deciduous
Dominican Republic, West Cordillera	Ic	20–25 Ma	0.92	0.80	Deciduous
Nicaragua	Ic	18–23 Ma	0.87	0.64	Deciduous
Malaysia, Borneo, Sarawak west.	II	15–17 Ma	0.94	0.64	Deciduous
Madagascar	Ic	from 10,000 to 50,000 yrs	0.82	0.59	Deciduous

* Chemical classification of fossil resins [3].

the difference in intensities between these bands in Ukrainian amber is much smaller. It can be assumed that the decrease in the absorption band at approximately 1645 cm^{-1} is a consequence of resin maturation [8, 12]. The ratio of the intensities $I(1650)/I(1450)$ of the studied resins is presented in Table 3.

In Figs 1 and 2, the spectra of some fossil resins show a change in the spectral profile in the wavenumber range $765\text{--}680\text{ cm}^{-1}$, which can be related to the band ratio values in the wavenumber ranges $1771\text{--}1543$ and $1510\text{--}1400\text{ cm}^{-1}$. In the spectra of fossil resins from Ukraine, France, the Dominican Republic and Nicaragua, band triplets are clearly visible at $744, 716$ and 694 cm^{-1} , $744, 725$ and 698 cm^{-1} , $744, 721$ and 696 cm^{-1} , and $744, 721$ and 696 cm^{-1} , respectively. The ratios of the areas $A(1650)/A(1450)$ and the intensities $I(1650)/I(1450)$ of all these fossil resins are similar, except that of the Nicaraguan resin, which has slightly lower intensities. The spectra of the Lebanese, Japanese and Mexican resins show a single broad peak at wavenumbers of $719, 723$ and 721 cm^{-1} , respectively. The ratios of the areas $A(1650)/A(1450)$ and the intensities $I(1650)/I(1450)$ of these resins are small, although the ages of their resins are different.

The shoulder (around 1465 cm^{-1}) near the 1440 cm^{-1} band is due to COH and CH_2 vibrations [15]

and is usually observed in recent resins, copals and fossil resins up to 50 million years old. Based on this observation, the disappearance of the band around 1465 cm^{-1} has also been suggested as an indication of resin maturation [22]. If diterpenoid components are present in an amber or copal sample, the $I1646/I1450$ ratio will be around 1.5 in immature samples and 0.4 in mature samples [8].

According to the data obtained from Figs 3 and 4, it can be assumed that the area ratios $A(1650)/A(1450)$ and intensity ratios $I(1650)/I(1450)$ of these fossil resins are directly dependent on the age of the resin. Since the Italian Dolomite resin is classified as resin class II [4, 3], and the remaining coniferous resins as resin class I, it is likely that this is why the intensity ratio $I(1650)/I(1450)$ of the Italian Dolomite resin does not follow the general trend.

FT-TIR spectroscopy

Fossil resins, due to their chemical structure, can be tentatively classified using infrared spectra based on the similarity of spectral shapes [13]. The wavenumber positions of the bands of the studied amber and other fossil resin samples and their vibrational assignments in the FT-IR spectra are presented in Table 4.

From the spectra presented in Fig. 5, it is noticeable that the most characteristic absorption range

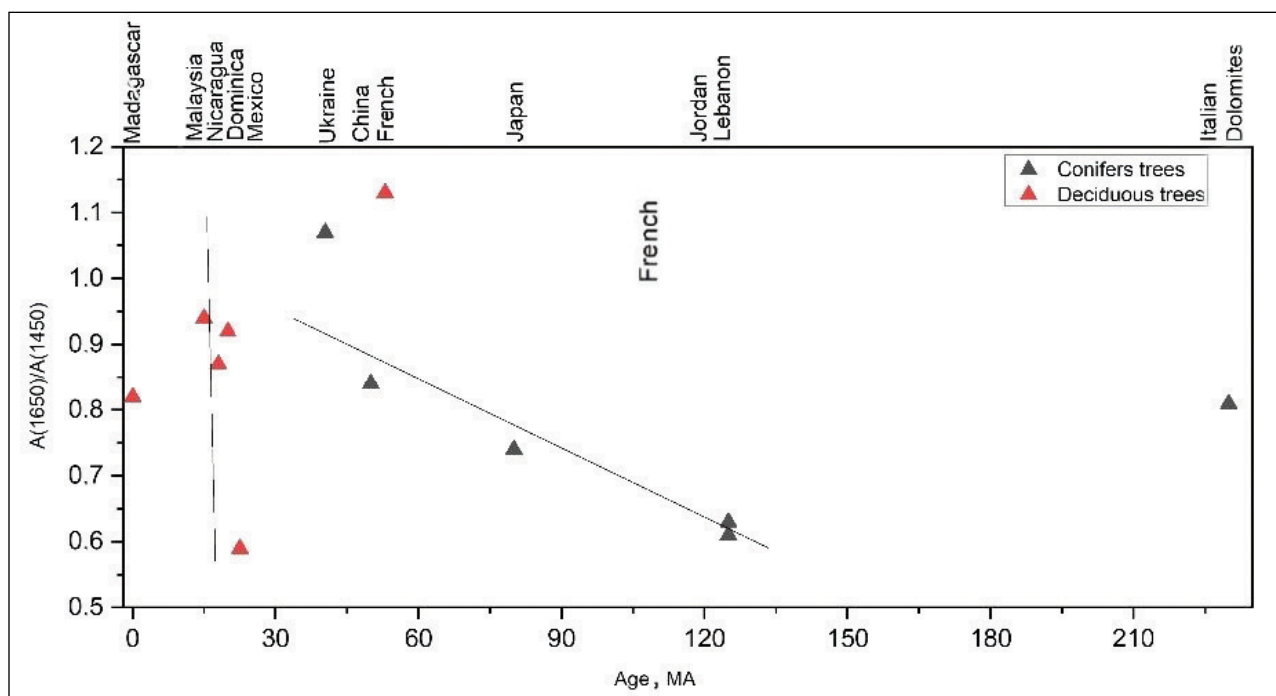


Fig. 3. Age dependence of the ratio of the areas of the studied resins $A(1650)/A(1450)$

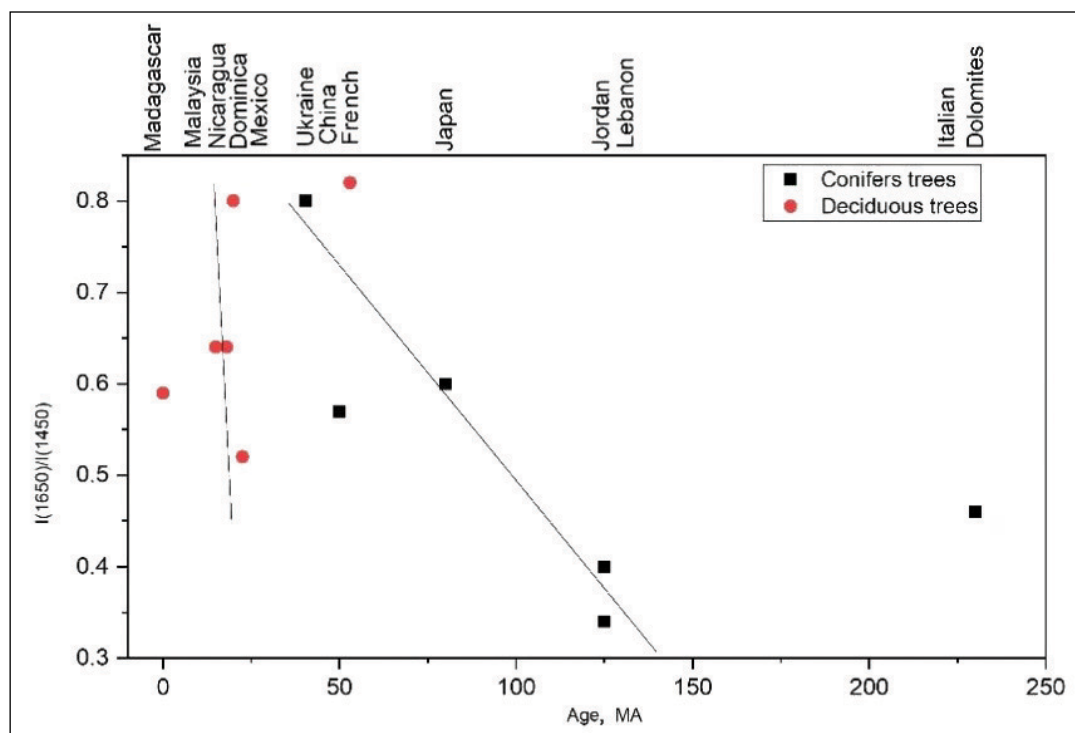


Fig. 4. Age dependence of the intensity ratio $I(1650)/I(1450)$ of the studied resins

Table 4. Infrared absorption band positions and assignments of fossil resins

Italian Dolomites	Jordan	Lebanon	Japan	China	Ukraine	French	Mexico	Dominica	Nicaragua	Malaysia, Borneo	Madagascar	Wavenumbers, cm^{-1}	References
									3078				
2926	2936	2923	2932	2927	2930	2929	2930	2929	2930	2933	2933	$\nu_{\text{asym}}(\text{CH}_3)$	
2869	2865	2868	2868	2868	2867	2867	2873	2868	2869	2871	2871	$\nu_{\text{sym}}(\text{CH}_3)$	
1706	1707	1704	1719	1720	1720	1701	1713	1716	1711	1700	1702	$\nu(\text{C}=\text{O})$	
1454	1455	1455	1454	1457	1456	1454	1455	1455	1457	1458	1456	$\delta(\text{CH}_2), \delta(\text{CH}_3)$	
1375	1375	1374	1379	1375	1374	1386	1381	1386	1387	1384	1376	$\delta(\text{CH}_2), \delta(\text{CH}_3)$	
					1247	1242		1242	1243			Baltic shoulder: $\nu(\text{C}=\text{O}),$ $\nu(\text{C}-\text{OH})$ in esters, carboxylic acids and tertiary alcohols	[*]
1228	1229	1232	1227	1225			1228				1228	$\delta(\text{CH}_2), \delta(\text{CH}_3),$ $\nu(\text{C}-\text{C}-\text{O})$	
						1173	1174	1174	1174			$\nu(\text{C}-\text{C}-\text{O})$	
1156	1156	1161	1163	1157	1161						1160	$\nu(\text{C}-\text{C}-\text{O})$	
1026	1030	1025	1033	1032	1020	1044	1042	1038	1040	1048	1026	$\nu(\text{C}-\text{O})$ in alcohols	
974	975	973		975		976		975			977	$\nu_{\text{oop}}(\text{C}=\text{C})$	
					888	886		888	887	885		$\nu_{\text{oop}}(\text{C}=\text{C})$	
853	853	852	856									$\delta_{\text{oop}}(\text{CH})$	
	814												

Abbreviations: oop, out-of-plane.

[*] <https://www.sciencedirect.com/science/article/pii/S1386142518301707>

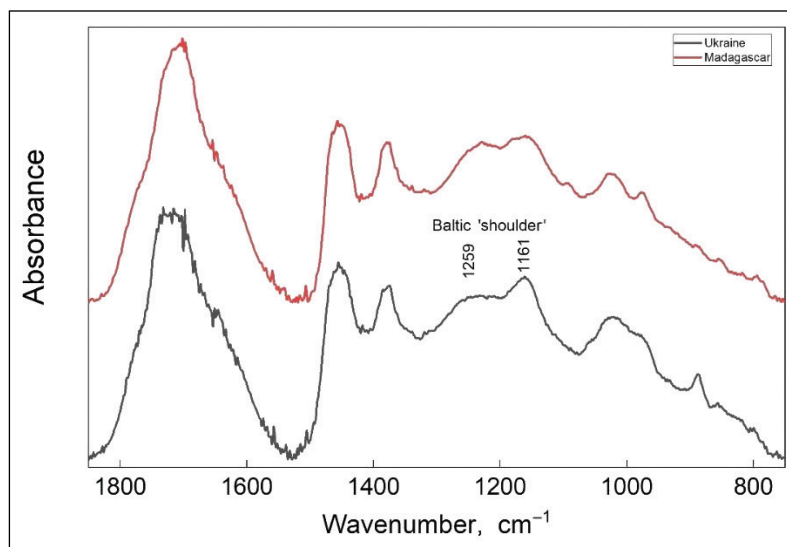


Fig. 5. Characteristic peak of the FT-IR spectrum of Baltic amber in the region of 1250–1175 cm^{-1}

is 1250–1150 cm^{-1} . The characteristic wavebands of this region, often called the ‘Baltic shoulder’, allow us to distinguish Baltic amber from other resins [18]. As stated in the article ‘Spectroscopic investigations of amber’, the 1161 cm^{-1} band is formed due to the stretching vibration of the C–O single bond of ester groups, probably amber esters, since its intensity varies depending on the intensity of the band due to the stretching vibration of the C=O double bond of the ester [6]. The brightest absorption band of Bal-

tic amber, related to the ester group at 1720 cm^{-1} , can be associated with the stretching of the C=O double bond of the carbonyl group. This band can also be formed when copal or other younger resins are exposed to air and light or heat [1].

When analysing the FTIR spectra of the test samples (Figs 6 and 7), it can be seen that in almost all spectra, weak peaks at 2369–2335 cm^{-1} are observed, which are attributed to atmospheric absorption of CO_2 .

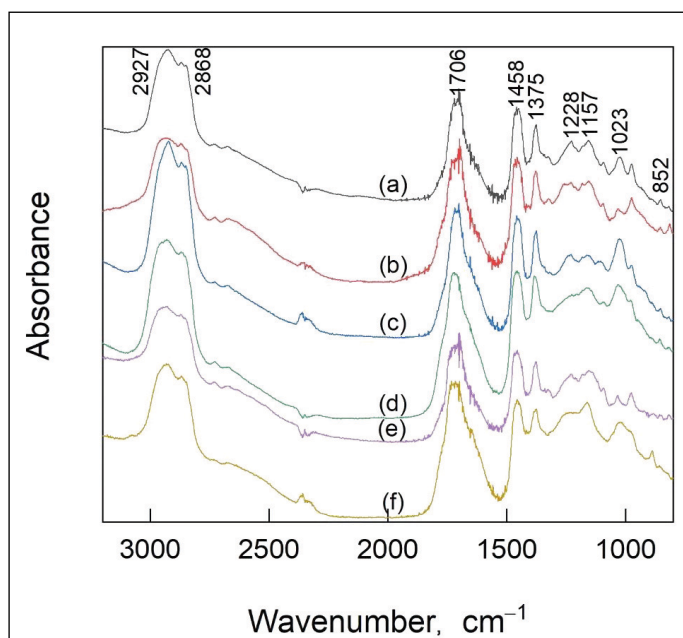


Fig. 6. FT-IR spectra of coniferous trees:
(a) Italy; (b) Jordan; (c) Lebanon; (d) Japan; (e) China; (f) Ukraine

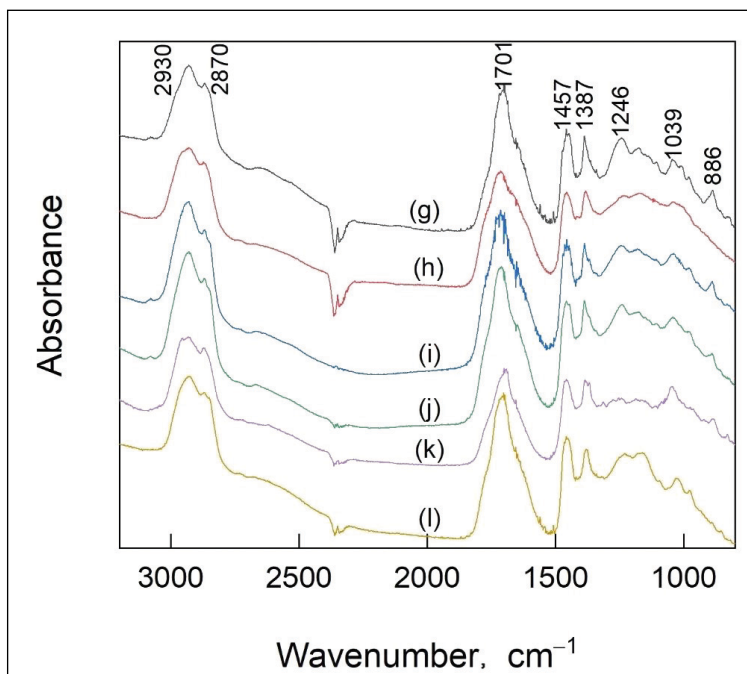


Fig. 7. FT-IR spectra of deciduous trees: (g) France; (h) Mexico; (i) Dominica; (j) Nicaragua; (k) Malaysia; (l) Madagascar

Despite the difference of tens or more millions of years between these fossil resins, the FT-IR spectra of all of them visually have a lot of similarities, except for Baltic amber (Fig. 6f). In none of the studied resins was the Baltic ‘shoulder’ observed in the spectrum of the resins examined. The prominent steep and narrow peak at 1700 cm^{-1} (in the $1500\text{--}1900\text{ cm}^{-1}$ region), which is attributed to the carbonyl group of esters, can provide information about the content of certain carbonyl compounds in the resins. It was observed that the intensity of the band associated with double bond vibrations decreases with resin aging, which can be a significant observation in assessing the age of the resin.

In all FT-IR spectra of the studied resins, peaks are observed in the absorption region of $1048\text{--}1020\text{ cm}^{-1}$, which are attributed to vibrations of the $\nu(\text{C}\text{--}\text{O})$ group. Based on these data, it can be concluded that the main components of these fossil resins are similar.

CONCLUSIONS

From the studies conducted, it can be concluded that it is very difficult to distinguish resins of different ages from different parts of the world based on the shape of Raman spectra. However, the ratios of the bands of fossil resin samples in the regions

$A(1650)/A(1450)$ and $I1646/I1450$ at $1771\text{--}1543$ and $1510\text{--}1400\text{ cm}^{-1}$ can help determine the degree of maturity of the resin, but the studied resins should be assigned to the same resin class. It can also help determine the geographical area where the resin originated.

In research, efforts should be focused on isolating the botanical source of the fossil resin, rather than its geographic location.

FT-IR spectroscopy is mainly focused on distinguishing resins from their imitations. However, this method has little use in classifying fossil resins or in trying to elucidate the chemical structure and the degree of maturity of the resin.

It has been confirmed that Baltic amber can be distinguished from other resins or their imitations by the characteristic bands at $1200\text{--}1260\text{ cm}^{-1}$ and 1700 , 1010 and 980 cm^{-1} observed in the FT-IR spectrum.

Since the resins under study can often be affected by processes such as impurities, aging or processing, further studies and evaluation of many more samples would be required when using FT-IR and Raman spectroscopy to determine the age and maturity of resins.

Received 27 March 2025

Accepted 22 April 2025

References

1. A. Abduriyim, H. Kimura, Y. Yokoyama, et al., *Gems Gemol.*, **45**(3), 158 (2009) [https://www.gia.edu/gems-gemology/fall-2009-green-amber-abduriyim].
2. K. B. Anderson, *Org. Geochem.*, **21**(2), 209 (1994).
3. K. B. Anderson, J. C. Crelling, *Amber, Resinite, and Fossil Resins*, ACS Symposium Series, Vol. 617, ix, American Chemical Society (1995).
4. K. B. Anderson, R. E. Winans, R. E. Botto, *Org. Geochem.*, **18**(6), 829 (1992) [https://doi.org/10.1016/0146-6380(92)90051-X].
5. G. I. Badea, M. C. Caggiani, P. Colomban, A. Mangone, *Appl. Spectrosc.*, **69**(12) (2015). DOI: 10.1366/15-07866.
6. C. W. Beck, *Appl. Spectrosc. Rev.*, **22**(1), 57 (1986) [https://doi.org/10.1080/05704928608060438].
7. C. W. Beck, E. Wilbur, S. Meret, D. Kossove, K. Kermani, *Archaeometry*, **8**(8), 96 (1965) [https://doi.org/10.1111/j.1475-4754.1965.tb00896.x].
8. R. H. Brody, G. M. Edwards, H. A. M. Pollard, *Spectrochim. Acta A Mol. Biomol. Spectrosc.*, **57**(6), 1325 (2001) [https://doi.org/10.1016/S1386-1425(01)00387-0].
9. S. Cebulak, A. Matuszewska, A. Langier-Kuzniarowa, *J. Therm. Anal. Calorim.*, **71**, 905 (2003) [https://doi.org/10.1023/A:1023390629412].
10. F. Czechowski, B. R. Simoneit, M. Sachanbiński, J. Chojcan, S. Wołowicz, *Appl. Geochem.*, **11**(6), 811 (1996) [https://doi.org/10.1016/S0883-2927(96)00046-7].
11. C. Dietz, G. Catanzariti, S. Quintero, A. Jimeno, *Archaeol. Anthropol. Sci.* **6**, 63 (2013). DOI: 10.1007/s12520-013-0129-4.
12. K. Drąg, M. Mroczkowska-Szerszeń, M. A. Dumanska-Słowik, Ż. Grażyna, *Spectrochim. Acta A Mol. Biomol. Spectrosc.*, **279**(5), 121404 (2022). DOI: 10.1016/j.saa.2022.121404.
13. P. Drzewicz, L. Natkaniec-Nowak, D. Czapla, *Trends Anal. Chem.*, **85**, Part C, 75 (2016) [https://doi.org/10.1016/j.trac.2016.06.022].
14. H. G. M. Edwards, M. J. Falk, *J. Raman Spectrosc.*, **28**, 211 (1997) [https://doi.org/10.1002/(SICI)1097-4555(199704)28:4<211::AID-JRS83>3.0.CO;2-1].
15. H. G. M. Edwards, D. W. Farwell, *Spectrochim. Acta A Mol. Biomol. Spectrosc.*, **52**(9), 1119 (1996) [https://doi.org/10.1016/0584-8539(95)01643-0].
16. M. Guiliano, L. Asia, G. Onorati, G. Mille, *Spectrochim. Acta A Mol. Biomol. Spectrosc.*, **67**(5), 1407 (2007). DOI: 10.1016/j.saa.2006.10.033.
17. J. Jehlička, S. E. J. Villar, H. G. M. Edwards, *J. Raman Spectrosc.*, **35**, 761 (2004) [https://doi.org/10.1002/jrs.1191].
18. A. Matuszewska, *Chemiczna budowa bursztynu (sukcynitu), Amberif 2012. Badania inkluzji i innych właściwości bursztynu*, Gdańsk (2012) [https://www.pgi.gov.pl/images/muzeum/kopalnia_wiedzy/surowce/foldery/bursztyn.pdf].
19. G. Pastorelli, Doctoral Thesis, University of Bologna (2009) [https://amsdottorato.unibo.it/2259/1/Pastorelli_Gianluca_tesi.pdf].
20. Z. F. Rao, K. Dong, X. Y. Yang, J. C. Lin, X. Y. Cui, R. F. Zhou, *Sci. China Phys. Mech. Astron.*, **56**(8), 1598 (2013). DOI: 10.1007/s11433-013-5144-z.
21. E. S. Teodor, E. D. Teodor, M. Virgolici, M. M. Manea, G. Truica, S. C. Litescu, *J. Archaeol. Sci.*, **37**, 2386 (2010) [https://doi.org/10.1016/j.jas.2010.04.011].
22. W. Winkler, E. Ch. Kirchner, A. Asenbaum, M. Musso, *J. Raman Spectrosc.*, **32**(1), 59 (2000) [https://doi.org/10.1002/1097-4555(200101)32:1<59::AID-JRS670>3.0.CO;2-D].

Gintarė Martinkutė-Baranauskienė, Martynas Talaikis,
Petras Šinkūnas, Jonas Kiuberis

**FT-IR IR RAMANO SPEKTROSKOPIJA GINTARO
IR KITŲ FOSILIJŲ DERVŲ TYRIMAMS**